The EMBO Journal Vol.16 No.20 pp.6066–6076, 1997

Mutations in the α1 subunit of an L-type voltage-activated Ca^{2+} channel cause myotonia in *Caenorhabditis elegans*

Raymond Y.N.Lee[1,2,3], Leslie Lobel[4,5], Michael Hengartner[4,6], H.Robert Horvitz[4] and Leon Avery[1]

[1]Department of Molecular Biology and Oncology, University of Texas Southwestern Medical Center, Dallas, TX 75235-9148 and [4]Howard Hughes Medical Institute, Department of Biology, Massachusetts Institute of Technology, Cambridge, MA 02139, USA

[2]Present address: Department of Genetics, Washington University School of Medicine, St Louis, MO 63110, USA
[5]Present address: Department of Medicine, Columbia University, New York, NY 10032, USA
[6]Present address: Cold Spring Harbor Laboratory, Cold Spring Harbor, NY 11724, USA

[3]Corresponding author
e-mail: raymond@genetics.wustl.edu

The control of excitable cell action potentials is central to animal behavior. We show that the *egl-19* gene plays a pivotal role in regulating muscle excitation and contraction in the nematode *Caenorhabditis elegans* and encodes the αl subunit of a homologue of vertebrate L-type voltage-activated Ca^{2+} channels. Semi-dominant, gain-of-function mutations in *egl-19* cause myotonia: mutant muscle action potentials are prolonged and the relaxation delayed. Partial loss-of-function mutations cause slow muscle depolarization and feeble contraction. The most severe loss-of-function mutants lack muscle contraction and die as embryos. We localized two myotonic mutations in the sixth membrane-spanning domain of the first repeat (IS6) region, which has been shown to be responsible for voltage-dependent inactivation. A third myotonic mutation implicates IIIS4, a region involved in sensing plasma-membrane voltage change, in the inactivation process.

Keywords: animal behavior/*Caenorhabditis elegans*/ muscle excitation/myotonia/voltage-activated calcium channel

Introduction

Regulation of action potential duration is important for excitable cell function. For example, in neurons, the duration of action potentials at the synaptic terminal can affect the amount of transmitter released (Hochner *et al*., 1986; Spencer *et al*., 1989), whereas in vertebrate cardiac and gastrointestinal smooth muscles the duration of action potentials modulates the duration and strength of contractions (Noble, 1979; Huizinga, 1991). The physiological importance of regulating the duration of action potentials is exemplified by the human cardiac Long QT Syndrome (LQTS), in which the prolongation of the QT interval on electrocardiograms reflects a delay in the repolarization of ventricular myocytes. LQTS can manifest itself in ventricular fibrillation and syncopal episodes, ultimately leading to the death of young, otherwise healthy individuals (Schwartz *et al*., 1995).

In ventricular myocytes there are at least three major ionic currents contributing to the action potential: a regenerative Na^+ current is responsible for fast depolarization, a Ca^{2+} current for the plateau phase and a K^+ current for repolarization of the membrane. The activation and inactivation kinetics of each of these currents can affect the duration of the action potential. Indeed, mutations in a cardiac Na^+ channel gene SCN5A and in a K^+ channel gene HERG have been shown to be the causes of two distinct forms of congenital LQTS (Curran *et al*., 1995; Wang *et al.*, 1995). Although many pharmacological and physiological studies have shown the importance of Ca^{2+} channels in shaping the cardiac action potential (Noble, 1979; Kass, 1995), mutations have not yet been found.

In general, the mechanisms regulating action potential duration are well conserved in metazoans. In recent years, it has been found that this mechanistic similarity extends to the molecular level. This conservation of molecular mechanisms has allowed physiologists to take advantage of the simplicity of invertebrates and their amenability to genetic approaches to help identify new molecules that are important for vertebrate excitable cell function. For example, the human HERG gene was cloned by its sequence homology to the *Drosophila ether-à-go-go* (*eag*) gene (Warmke and Ganetzky, 1994). The *eag* gene was identified because of its effect on fruit fly neural and muscle functions when mutated (Zhong and Wu, 1991).

We are studying the control of muscle action potential duration at the molecular level by analyzing a simple neuromuscular pump, the pharynx of the nematode *C.elegans*. The pharynx, consisting of 20 myoepithelial muscle cells, 20 neurons and 22 other structural and secretory cells, is the feeding organ of the nematode. The muscles are arranged radially around a lumen, so that contraction opens the lumen and relaxation closes it. In the anterior pharynx, corpus muscle contraction serves to take in food (bacteria) suspended in liquid, whereas relaxation expels the liquid while trapping the food. In the posterior pharynx, terminal bulb muscle contraction rotates a grooved cuticular structure called the grinder that grinds bacteria and passes debris towards the intestine. Relaxation returns the grinder to its resting position. A pump is a cycle of nearly synchronous contraction and relaxation of the corpus and the terminal bulb (Albertson and Thomson, 1976; Avery and Horvitz, 1989).

The pharyngeal muscles are the most experimentally accessible excitable tissue in *C.elegans*. Pharyngeal electrical activity can be monitored in living animals by a simple extracellular recording called the electropharyngeogram (EPG; Raizen and Avery, 1994). The pharynx can

be dissected from the rest of the animal, allowing pharmacological manipulation and direct measurement of muscle action potentials by intracellular recording (Davis *et al.*, 1995). Similar to vertebrate cardiac and some smooth muscles, pharyngeal muscles can have myogenic activity (Avery and Horvitz, 1989). Contraction and relaxation are tightly correlated with the depolarization and repolarization phases of muscle action potentials. An action potential normally lasts about 150 ms (Raizen and Avery, 1994; Davis *et al.*, 1995; Starich *et al.*, 1996).

We have analyzed mutations that affect the duration of the pharyngeal muscle action potential. We find that *egl-19* encodes the α1 subunit of a putative voltage-activated Ca^{2+} channel that is probably of the L type. Gain-of-function mutations in *egl-19* cause prolonged muscle action potentials and contractions (myotonic class), reduction-of-function mutations cause a reduced rate of depolarization and feeble contractions (flaccid class), and severe loss-of-function mutations lead to a complete loss of muscle contraction and thus lethality (lethal class). We have localized two myotonic mutations in the IS6 (the sixth membrane-spanning domain in the first repeat) region and flanking residues. This region has been shown to control the rate of the voltage-dependent inactivation between different types of Ca^{2+} channels (Zhang *et al.*, 1994). We also found one myotonic mutation in IIIS4 (the fourth membrane-spanning domain in the third repeat), a region that is a voltage sensor for channel activation (Catterall, 1995). Our results demonstrate the importance of a voltage-activated Ca^{2+} channel in regulating the duration of action potentials. Furthermore, our mutant analysis suggests that the IS6 and IIIS4 regions play a role in L-type Ca^{2+} channel inactivation.

Results

Three classes of egl-19 mutations affect muscle contraction and excitation

There are at least 26 mutant alleles of the *egl-19* gene (Table I, see Materials and methods for mutant isolation). These mutant alleles can be classified into three groups based on their genetic and phenotypic characteristics. The myotonic class of mutations causes a semi-dominant excessive muscle contraction phenotype, which is a result of increased or misregulated gene activity. The flaccid class of mutations causes a recessive feeble muscle contraction phenotype which results from a partial reduction of gene function. The lethal mutations are recessive and cause a near-complete block of embryonic muscle contraction as a consequence of a severely reduced or absent gene function. The inability of embryonic body muscles to contract leads to a distinctive embryonic lethal phenotype referred to as the Pat (Paralyzed, Arrested elongation at Two-fold) phenotype (Williams and Waterston, 1994).

Myotonic mutations

Three mutations, *n2368sd*, *ad695sd* and *ad952*, are in the myotonic class. In an *n2368sd* mutant pharynx, the terminal bulb muscles, but not those of the corpus, often showed dramatically delayed relaxation (Figure 1A). To see whether the delay in relaxation was caused by delayed repolarization of muscle action potentials, we measured the electrical activities of the pharyngeal muscles by recording EPGs from intact worms. EPGs are analogous, in principle, to electrocardiograms or electroencephalograms used on humans. The EPG method provides a measurement of the capacitative current flows associated with changes in transmembrane potentials of pharyngeal muscle cells (Raizen and Avery, 1994). Thus, during a pump, fast depolarization of corpus and terminal bulb muscles in near-synchrony together causes a group (usually a pair) of upward transients in EPG. Repolarization of the corpus produces a large downward transient followed by a smaller downward transient caused by the repolarization of the terminal bulb (Figure 1B; Raizen and Avery, 1994). EPGs showed that *n2368sd* mutant worms had terminal bulb muscle action potentials that were dramatically prolonged (one example is shown in Figure 1B). Delayed relaxation of the terminal bulb in *n2368sd* mutants is consistently associated with a delay in terminal bulb muscle repolarization (data not shown). This correlation between muscle relaxation and repolarization defects suggests that the muscle relaxation defect is caused at least in part by the repolarization defect. Consistent with their normal corpus muscle contractions, EPGs did not reveal a defect in corpus electrical activities in *n2368sd* mutant animals (Figure 1B). Nevertheless, *n2368sd* mutant animals also showed hypercontraction of several other muscles. They had a short and dumpy morphology (Figure 2A), possibly caused by excessive body muscle tone, and they were egg-laying constitutive (Figure 2F), apparently because of excessive contraction of the egg-laying muscles, as the frequency and duration of vulval muscle contractions were increased (data not shown). The *n2368sd* mutation is semi-dominant. *n2368sd*/+ heterozygous animals had similar but weaker myotonic defects than those seen in homozygous mutant animals (data not shown).

ad695sd, like *n2368sd*, causes a semi-dominant myotonic phenotype, although its defects are generally weaker than those of *n2368sd* animals (Table 1; Avery, 1993). Intracellular measurement of *ad695sd* terminal bulb muscle action potentials from two animals confirmed that *ad695sd* causes prolonged plateau phases (Figure 1C), as had been concluded earlier on the basis of EPGs (Raizen and Avery, 1994).

The *ad952* mutation was isolated in a genetic screen for dominant suppressors of *egl-19*(*n582*) (see Materials and methods). *ad952* is tightly linked to *n582* (within one map unit, see Materials and methods) and was shown by sequencing (see below) to be in *egl-19*. *n582 ad952* double mutant animals were essentially wild-type in phenotype except that they were slightly dumpy, and the pharyngeal terminal bulb occasionally showed delayed relaxation and repolarization (Table I and data not shown). These phenotypes are similar to but much weaker than those seen in either *n2368sd* or *ad695sd* animals. *n582 ad952*/+ heterozygotes are wild-type, unlike *n2368sd*/+ and *ad695sd*/+ heterozygotes. These results suggest that *egl-19*(*n582 ad952*) is a weak gain-of-function mutant.

Flaccid mutations

egl-19 flaccid mutants have feeble muscle contractions of both the corpus and the terminal bulb in the pharynx (Figure 1A). Their EPGs were normal with respect to the timing and amplitude of major signal peaks (Figure 1B). However, intracellular measurement of terminal bulb

Table I. Summary of *egl-19* mutations

Class	Mutations	Phenotypes				
		Pharyngeal	Body	Egg-laying	Male mating[a]	Embryonic[b]
Myotonic	*n2368sd*	terminal bulb relaxation-defective	dumpy[c], slightly jerky movement	constitutive, suppresses HSN^-	protruding spicules	cold-sensitive Pat
	ad695sd[d]	terminal bulb relaxation-defective	slightly dumpy	weakly constitutive	protruding spicules	normal
	n582 ad952	slight terminal bulb relaxation-defective	slightly dumpy	normal	normal	normal
Flaccid	*n582*[e]	feeble pumping	long and thin, slow and floppy	defective[e]	unable to protrude spicules[f]	normal
	ad1006, *ad1013*, *ad1015*, *ad995*,	feeble pumping	long and thin, slow and floppy	defective	nd	normal
	ad1025	feeble pumping leading to larval lethality	slightly slow	nd	nd	normal
Lethal	*ad980*, *ad991*,	feeble pumping	variably bulged[g]	defective	nd	occasional Pat
	ad993, *ad1004*, *ad1008*, *ad1009*, *ad1017*, *st553*[h], *st556*, *st569*, *st571*, *st576*, *st577*,	nd	nd	nd	nd	Pat
	n2368sd ad1023,	nd	nd	nd	nd	Pat
	ad695sd ad1000, *ad695sd ad1002*, *ad695sd ad1021*	nd	nd	nd	nd	Pat

nd: not determined.
[a]During mating, the male copulatory spicules are inserted into the vulva of the hermaphrodite by means of the protractor muscles (Hodgkin, 1988).
[b]Pat (paralyzed, arrested elongation at 2-fold) phenotype refers to a specific embryonic lethal phenotype shared by many mutants defective in muscle genes, described by Williams and Waterston (1994). *n2368sd* mutants showed embryonic phenotype only at low (<15°C) temperatures (see text).
[c]Short, contracted morphology.
[d]Previously described by Avery (1993) as *eat-12*.
[e]Previously described by Trent *et al.* (1983).
[f]K.S.Liu, personal communication.
[g]This phenotype is apparently a less expressive Pat-like phenotype.
[h]The *st* alleles were previously described by Williams and Waterston (1994) as *pat-5*.

muscle action potentials in *n582* (eight individuals, one typical action potential shown in Figure 1C) and *ad995* (not shown) animals revealed that the rate of depolarization was reduced, suggesting that *egl-19* has a role in bringing about fast depolarization. In addition to the pharyngeal phenotype, flaccid mutants showed feeble body wall and egg-laying muscle contractions. They tend to be long and thin, slow in movement and are egg-laying defective (Figure 2C and H; Trent *et al.*, 1983).

Lethal mutations

The lethal class of *egl-19* mutants has the Pat phenotype (Figure 2D and E). There was a dramatic reduction in the extent and frequency of embryonic body muscle contractions, and the most severe mutants did not contract at all (Williams and Waterston, 1994; data not shown). Embryonic body wall muscle contractions are apparently myogenic (Hall and Hedgecock, 1991; L.Avery, unpublished observations). Mutations in many genes important for muscle structure or function (for instance, those that encode myosin heavy chain A, vinculin, tropomyosin or troponin C) have the Pat phenotype (Williams and Waterston, 1994, and references therein), but no mutations in genes that affect only nervous system function have been found to have a Pat phenotype. The fact that the strongest alleles of *egl-19* eliminated embryonic muscle contraction suggests that *egl-19* affects embryonic muscle function directly rather than through the nervous system.

We conclude, based on mutant phenotypes, that the normal activity of *egl-19* is necessary for muscle depolarization and for regulating the duration of muscle action potentials.

Cloning of a *C.elegans* homolog of α1 subunits of vertebrate L-type voltage-activated Ca^{2+} channels

Genetic mapping data (Trent *et al.*, 1983; Avery, 1993; Williams and Waterston, 1994; and Materials and methods) positioned *egl-19* in a small genetic interval between *deb-1* and *dif-1* on linkage group (LG) IV. This interval corresponds to a physical distance of approximately 150 kb in which we found a putative Ca^{2+} channel gene in independent experiments.

Specifically, by degenerate PCR (polymerase chain reaction), we cloned from *C.elegans* a cDNA fragment corresponding to the IIIS6–IVS6 region (from the sixth membrane-spanning segment of the third repeat to the sixth membrane-spanning segment of the fourth repeat) of known vertebrate voltage-activated Ca^{2+} channel α1 subunits. We extended the sequence of the putative Ca^{2+} channel gene by screening a *C.elegans* cDNA library

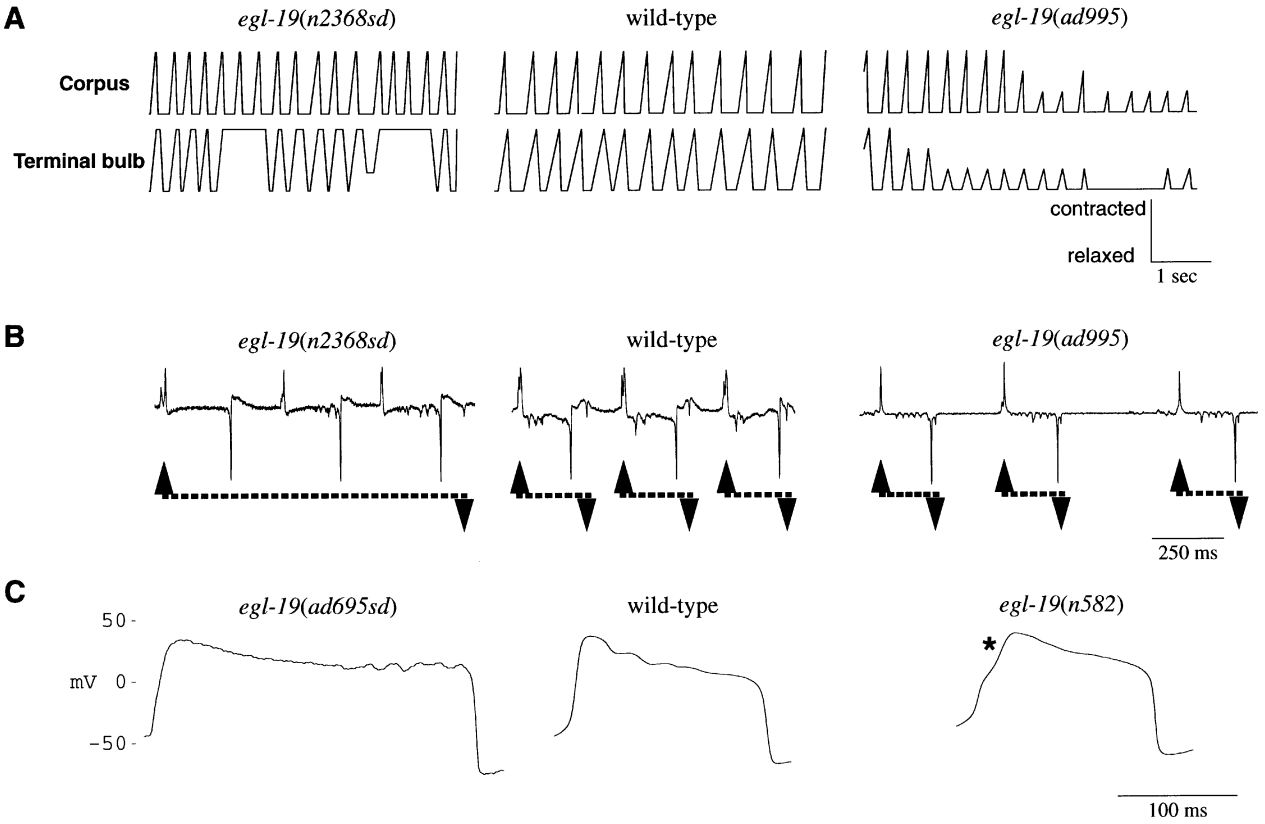

Fig. 1. Pharyngeal muscle contraction and electrical phenotypes of wild type and *egl-19* mutants. (**A**) Timing diagrams schematically represent the pumping motion. Each of the three panels represents the pumping motion of a single animal analyzed by observation of video records frame-by-frame. The horizontal (time) scale has a resolution of 1/60 s, whereas the vertical scale (extent of contraction) is qualitative (Avery, 1993). The pumping motions shown are representive of animals of each of the genotypes, respectively. In the *n2368sd* mutant, terminal bulb muscle contractions last longer than those in the wild type. In the *ad995* mutant, both corpus and terminal bulb muscle contractions are often feeble and incomplete. The wild-type diagram is reproduced with permission from Avery (1993). (**B**) EPG recordings of pharyngeal muscle action potentials. For each genotype, an ~1200 ms stretch of a typical EPG recording is shown. The upward arrowheads mark the timing of peaks representing terminal bulb muscle depolarizations and the downward arrowheads mark the timing of repolarization transients. The duration of a terminal bulb muscle action potential is represented by a dashed line. The terminal bulb muscle depolarization peaks usually coincide with those of the corpus, often as a doublet (Raizen and Avery, 1994). The terminal bulb repolarization transients are the small ones following the larger transients generated by the corpus muscles. (**C**) Intracellular recordings from terminal bulb muscles. *ad695sd* mutant muscles have occasional action potentials with significantly prolonged plateau phases. One such action potential is shown here. This phenotype agrees with that observed in *ad695sd* EPG measurements (Raizen and Avery, 1994). Terminal bulb muscle action potentials in *n582* mutants routinely show slow kinetics during the depolarization phase. One such action potential is shown with an asterisk marking the slow phase.

and by multiple steps of reverse transcriptase-coupled polymerase chain reaction (RT–PCR; see Materials and methods). We analyzed the presumptive ORF (open-reading frame) of this putative Ca^{2+} channel gene (Figure 3A) by comparing its sequence to available protein sequences in databases and found that it is significantly more similar to known α1 subunits of L-type channels than to other types of voltage-activated Ca^{2+} channels (Figure 3B). Furthermore, this putative Ca^{2+} channel has most (19 out of 23) of the otherwise absolutely conserved amino acid residues found in domains IIIS5-S6 and IVS5-S6 of α1 subunits of known L-type Ca^{2+} channels (Figure 3C). IIIS5-S6 and IVS5-S6 are two regions implicated in mediating channel sensitivity to 1,4-dihydropyridines (Grabner *et al.*, 1996). Dihydropyridine sensitivity is the defining characteristic of L-type Ca^{2+} channels. In fact, pharyngeal muscles are sensitive to nifedipine, a dihydropyridine: nifedipine-treated dissected pharynx showed feeble muscle contraction with an extended action potential (J.A.Dent, personal communication). Other muscles in *C.elegans*, for example body muscles, are also sensitive to L-type Ca^{2+} channel blockers (L.Lobel and H.R.Horvitz, unpublished observations). Because of the high degree of sequence similarity, we believe that we have cloned the α1 subunit of a *C.elegans* L-type Ca^{2+} channel.

We mapped the physical location of this Ca^{2+} channel gene to cosmid C48A7 by hybridizing the cloned cDNA fragment to a YAC grid, and subsequently to cosmids covered by the positive YAC clones (see Materials and methods). By comparing its sequence to the recently released C48A7 cosmid sequence (for a description of the *C.elegans* genomic project, see Wilson *et al.*, 1994), we found that the Ca^{2+} channel gene lies completely within C48A7 (Figure 4).

egl-19 encodes a voltage-activated Ca^{2+} channel

C48A7 is between the genes *deb-1* and *dif-1* on LGIV, consistent with the location of the *egl-19* gene. We considered the possibility that *egl-19* is the Ca^{2+} channel gene, since *egl-19* mutant phenotypes are suggestive of defective muscle Ca^{2+} channels.

By germline transformation rescue experiments, we

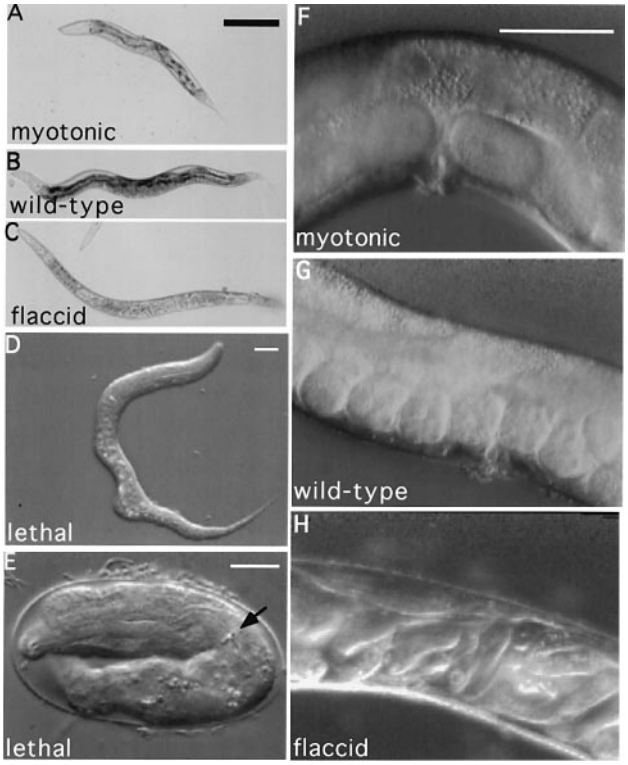

Fig. 2. Morphology and egg-laying phenotypes of the wild type and *egl-19* mutants (**A**) Dumpy morphology of a myotonic mutant *n2368sd*. (**B**) Morphology of the wild type. (**C**) Long and thin morphology of a flaccid mutant *ad995*. The mutants have the pale appearance generally seen in feeding-defective mutants (Avery, 1993). Scale bar = 200 μm. (**D**) Variable lumpy morphology of an *ad980* mutant L1 larva, indicating incomplete morphogenesis, probably caused by reduced embryonic muscle contraction. Scale bar =10 μm. (**E**) An *ad980* mutant arrested as a two-fold embryo with a well-developed pharynx (grinder marked by an arrow), a typical phenotype of Pat mutants (Williams and Waterston, 1994). Scale bar = 10 μm. (**F**)–(**H**) Micrographs showing the uterus in mutant and wild-type animals. These animals were of a similar age (within two days after the L4 molt). Eggs in the uterus were at a much earlier embryonic stage (fewer cells) in (F), an *n2368sd* mutant hermaphrodite, than in (G), a wild type, indicating an egg-laying constitutive phenotype. (H) In contrast, late-stage embryos that were about to hatch were retained by an *ad995* mutant mother, indicating an egg-laying defective phenotype. Scale bar = 50 μm.

found that transgenic *egl-19*(*n582*) mutant animals bearing the C48A7 transgene showed a nearly wild-type phenotype with respect to pharyngeal, body and egg-laying muscle contractions, suggesting that C48A7 contains sequences necessary for *egl-19* gene activity. By mapping the extent of the *egl-19* rescuing activity within C48A7, we found that the rescuing activity is co-extensive with the Ca^{2+} channel gene (Figure 4).

To confirm that *egl-19* encodes the Ca^{2+} channel and to identify the molecular lesions in *egl-19* mutants, we determined the sequences of the entire coding regions of the Ca^{2+} channel in three *egl-19* mutants: the two myotonic mutants *ad695sd* and *n2368sd*, and the double mutant *n582 ad952*, which carries a flaccid mutation *n582* and a myotonic mutation *ad952*. For each of these mutations we found a corresponding single-base G:C→A:T transition in the coding sequence (Figure 3A). The *ad695sd* mutation changes alanine 906 in IIIS4 to a valine. In *n2368sd*, glycine 365 near the cytoplasmic end of IS6 is changed to an arginine. Two mutations were found in the *n582 ad952* double mutant. Since the *n582 ad952* double mutant was derived directly from an *n582* single-mutant animal, we were able to identify which of the two mutations found in the double mutant was *n582* by determining the sequences of the two mutation sites in DNA isolated from *n582* single-mutant animals. The *n582* mutation is in IIIS4 and changes arginine 899 to a histidine. The *ad952* mutation changes serine 372 to a leucine close to the predicted intracellular end of IS6. The fact that there is a mutation in Ca^{2+} channel coding sequence corresponding to each of the four identified *egl-19* mutations, and that the *egl-19* rescuing activity is co-extensive with the Ca^{2+} channel gene in the genomic sequence, argues strongly that the Ca^{2+} channel and *egl-19* are the same gene.

egl-19 is expressed and functions in muscle cells

Although it is clear from mutant phenotypes that *egl-19* affects excitation and contraction of muscles, *egl-19* could nevertheless be influencing muscles indirectly, e.g. through the nervous system. To address the question of how *egl-19* affects muscle excitation, we localized its expression by assaying the expression of an *egl-19*::*GFP* (green fluorescent protein, Chalfie *et al.*, 1994) reporter (Figure 4). In transgenic animals carrying the fusion gene, an *egl-19*::*GFP* fluorescent signal was first detected in body wall muscles in 1–1/2-fold embryos (Figure 5A and B), before the onset of embryonic muscle contraction. This result is consistent with the Pat phenotype seen in lethal mutants, suggesting a cell-autonomous muscle defect. By the time of hatching, *GFP* fluorescence was found in pharyngeal muscles pm3, pm4, pm5 and pm7 (Figure 5C), in body wall muscles (Figure 5F) and in the anal depressor muscle (Figure 5D and E). The muscle expression pattern is again consistent with a muscle cell-autonomous defect caused by mutations. We also found expression in the nervous system, including the pharyngeal neuron M4 and several neurons in the head, the ventral nerve cord and the pre-anal ganglion (Figure 5C and E, and data not shown). This expression pattern suggests that *egl-19* may also function in neurons (see Discussion).

In the wild type, the HSN neurons are required for normal egg-laying muscle contraction (Trent *et al.*, 1983). We found that egg-laying muscles in *egl-19*(*n2368sd*) myotonic mutants contract even in the absence of HSN motor neurons (see Materials and methods). This observation suggests that *egl-19* acts in egg-laying muscles to promote contraction. However, we could not detect GFP expression in egg-laying muscles. The promoter fragment we used probably lacks elements for egg-laying muscle expression (see Figure 4 and Materials and methods).

Discussion

We have identified three classes of *egl-19* mutations. Mutations that belong to each of the classes have been isolated previously. We now know that *egl-19*(*n582*), isolated by Trent *et al.* (1983), is a flaccid, partial loss-of-function allele, and *eat-12*(*ad695sd*), isolated by Avery (1993), is a myotonic, gain-of-function allele. Six alleles of *pat-5* were isolated by Williams and Waterston (1994). These alleles are *egl-19* lethal, severe loss-of-function or null mutations (B.Williams, personal communication; see also Materials and methods). The phenotypes of these

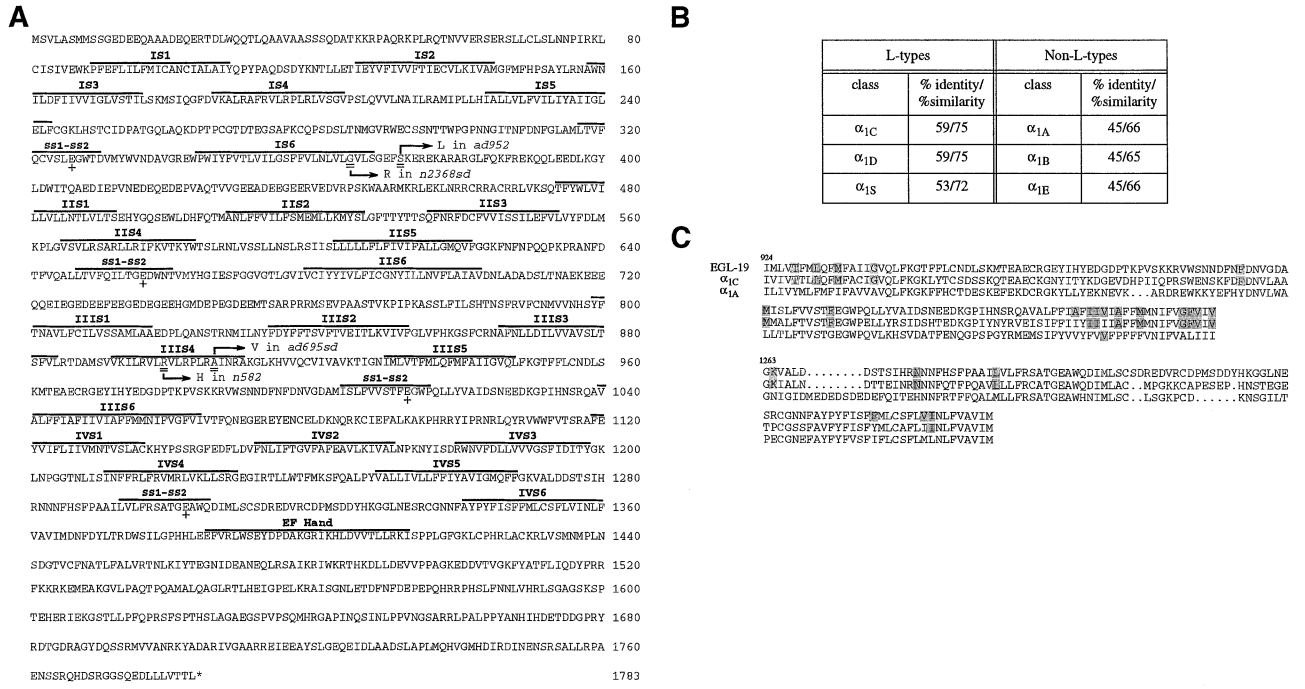

Fig. 3. EGL-19 Ca^{2+} channel sequence and comparisons with known Ca^{2+} channels. (**A**) The largest ORF predicted from the Ca^{2+} channel cDNA sequence is shown. This polypeptide of 1783 amino acids has all the hallmarks of αl subunits of voltage-activated Ca^{2+} channels (Catterall, 1995). Marked features in the sequence are based on sequence alignment analysis to known L-type Ca^{2+} channel genes (referenced in part B). There are four imperfect internal repeats (I–IV), each with six potential membrane-spanning helices (S1–S6, marked on top of the segments). Each repeat has a segment that is thought to line the channel pore (marked as SS1-SS2). Within each SS1-SS2 segment, there is a glutamate residue (marked by a '+' underneath) that is involved in coordinating the Ca^{2+} ion in the pore (Catterall, 1995). An EF-hand (consensus Ca^{2+}-binding site marked by a line above) is found in the predicted cytoplasmic tail, as in known Ca^{2+} channels (de Leon *et al*., 1995). Bent arrows and double underlines mark the predicted amino acid substitutions found in four *egl-19* mutant alleles (see text). (**B**) Sequence comparisons of EGL-19 to six different classes of vertebrate Ca^{2+} channel α1 subunits: $\alpha1_A$ (Mori *et al*., 1991), $\alpha1_B$ (Williams *et al*., 1992a), $\alpha1_C$ (Mikami, *et al*., 1989), $\alpha1_D$ (Williams *et al*., 1992b), $\alpha1_E$ (Niidome *et al*., 1992) and $\alpha1_S$ (Grabner *et al*., 1991). (**C**) Sequence comparison of EGL-19 to an L-type and a non-L-type Ca^{2+} channel within the regions IIIS5–IIIS6 and IVS5–IVS6, responsible for dihydropyridine sensitivity. In these regions, 23 residues (highlighted in EGL-19 sequence) are identical among all previously known L-type channels and among all known non-L-type channels, but different between L- and non-L-types (Grabner *et al*., 1996). Of these 23 residues, EGL-19 has 19 identical to L-type and only one identical to non-L-type. In three cases EGL-19 is different from both L-type and non-L-type. The sequence of *egl-19* has been deposited in GenBank under the accession No. AF023602.

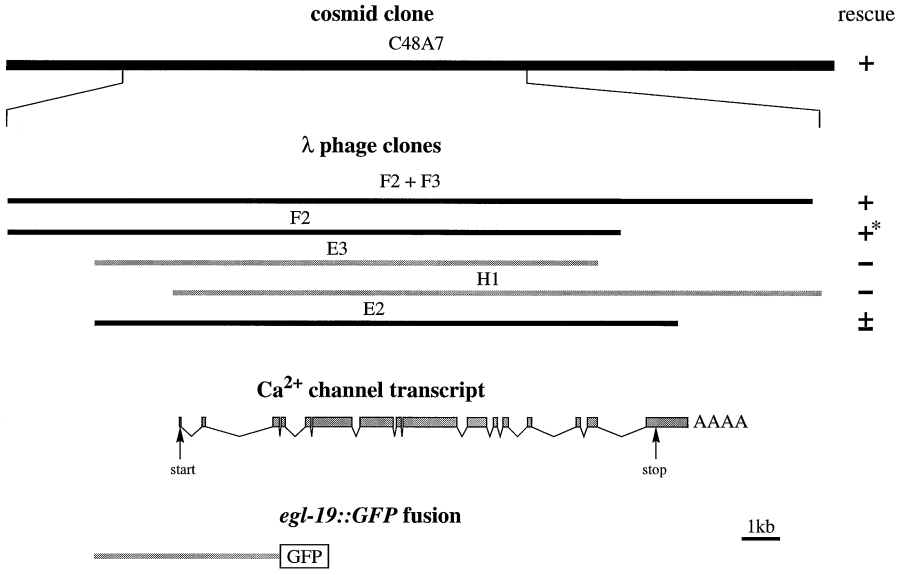

Fig. 4. Molecular localization of *egl-19*. This figure summarizes our strategy and results in defining the minimal genomic region that contains *egl-19*(+) and its relationship to the Ca^{2+} channel gene. Inserts of the genomic λ phage clones were mapped with respect to the cosmid C48A7. The ability of each genomic clone to rescue *egl-19*(*n582*) mutants was tested by germline transformation (see Materials and methods for detail). The E2 clone can rescue both pharyngeal and the body muscle defects but not the egg-laying defect. The last line shows the extent of the genomic fragment used to construct the *egl-19*::*GFP* fusion. *Although most transgenic animals carrying the F2 clone were rescued to an essentially wild-type phenotype, some acquired a new pharyngeal defect not seen in the controls (see Materials and methods).

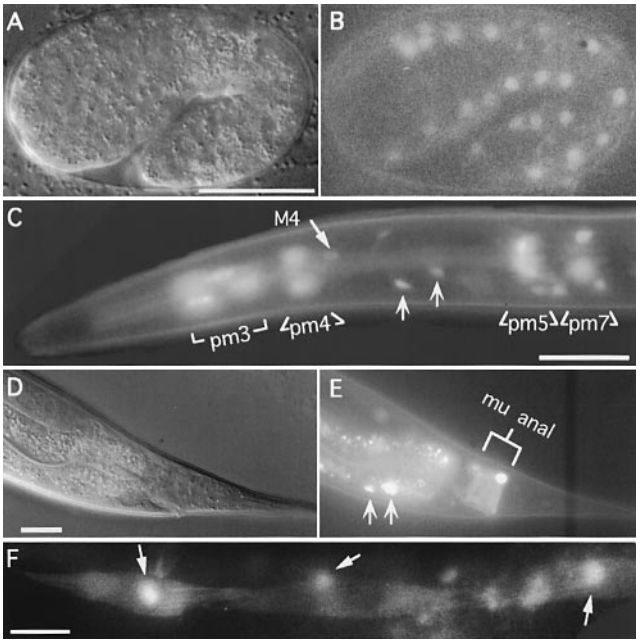

Fig. 5. Expression of an *egl-19*::*GFP* fusion construct in transgenic animals. The fusion gene contains a nuclear localization signal so that the fluorescent signal is most concentrated in nuclei, although a less intense signal can be seen in the cytoplasm. (**A**) Differential interference contrast (DIC) and (**B**) fluorescent views of a 1–1/2 fold embryo. The bright dots in (B) are two rows of body wall muscle nuclei expressing GFP. Scale bar = 20 μm. (**C**) GFP fluorescent signal is found in pharyngeal muscles pm3, pm4, pm5 and pm7. The signal is also found in a number of neurons. For example, M4 in the pharynx is marked by a plain arrow and two neurons in the anterior nerve ring are marked by barbed arrows. (**D**) DIC and (**E**) fluorescent views of the tail of an adult hermaphrodite. Expression is found in anal depressor muscles (mu anal); barbed arrows mark the nuclei of two neurons in the pre-anal ganglion. (**F**) Fluorescent signal from three adult body wall muscle cells. The nuclei are marked by arrows.

three classes of mutants considered together speak to the pivotal role that *egl-19* plays in muscle excitation and contraction.

Nematode pharyngeal muscles are similar to vertebrate cardiac and mammalian gastrointestinal smooth muscles that have slow-wave-type action potentials in several respects. For example, these types of muscles depolarize and contract cyclically; their action potentials have a long plateau phase; and the timing of contraction and relaxation is correlated to the depolarization and repolarization of their action potentials, respectively (Noble, 1979; Huizinga, 1991; Raizen and Avery, 1994; Davis *et al.*, 1995). In vertebrates, L-type voltage-activated Ca^{2+} channels are known to be important in regulating the excitation and contraction of cardiac myocytes (Bean, 1989). Similarly, L-type channels have been implicated in the slow-wave-type action potentials in mammalian gastrointestinal smooth muscles (Huizinga, 1991). Our results show that a putative L-type voltage-activated Ca^{2+} channel encoded by the *egl-19* gene serves a similar function in *C.elegans* pharyngeal muscles. These observations suggest that the nematode pharynx may be a good model system in which to study how varying Ca^{2+} channel activity may affect the physiology of muscles that have long action potentials.

egl-19 encodes the major Ca^{2+} channel in C.elegans muscles

Most *C.elegans* muscles are sensitive to *egl-19* gene activity, including embryonic and post-embryonic body wall muscle, pharyngeal muscle, egg-laying muscle and possibly anal depressor and male spicule protractor muscle (Table 1; Figure 5). Therefore, EGL-19 is the α1 subunit of a major muscle voltage-activated Ca^{2+} channel in *C.elegans*. To date, only one other voltage-activated Ca^{2+} channel αl subunit has been genetically characterized (Schafer and Kenyon, 1995). In contrast to *egl-19*, *unc-2* encodes an α1 subunit more similar to non-L than L-type voltage-activated Ca^{2+} channels. Reduction of *unc-2* function leads to an egg-laying constitutive phenotype, opposite to that of *egl-19* reduction-of-function. Furthermore, *unc-2* primarily affects neural function (Schafer and Kenyon, 1995; Schafer *et al.*, 1996). *unc-2*, however, does have a functional role in body muscles. *unc-2* mutants are sluggish in movement, and based on mosaic studies, Schafer and Kenyon (1995) concluded that this phenotype is caused by the loss of *unc-2* function in body muscles. Thus, although our data suggest that *egl-19* is functionally the major voltage-activated Ca^{2+} channel in muscles, other Ca^{2+} channels may also contribute to muscle excitation and contraction.

The expression pattern of an *egl-19*::*GFP* reporter indicates that *egl-19* is also expressed in many neurons. We do not know the functional significance of the nervous system expression, since most of the defects of *egl-19* mutants are consistent with defects in muscle function exclusively. However, muscle defects would mask most nervous system defects. One exception is that *ad695sd* and *n2368sd* animals have a dauer-formation defect (Daf-d). A dauer larva is an enduring, dispersal form of larva that is of a developmental stage equivalent to an L3. Although some dauers did develop from starved *ad695sd* or *n2368sd* mutant L2 larvae, many of these dauer animals appeared to be incompletely modified, as they were less resistant to SDS treatment than wild-type dauers (data not shown). Normal dauers have modified cuticles which render them resistant to harsh environmental conditions (Riddle, 1988). Since the formation of dauers is largely dependent on neural function (Riddle, 1988), and no mutations affecting only muscle function have been reported to cause a dauer-formation defect, this Daf-d phenotype suggests that *egl-19* may also function in the nervous system.

Control of pharyngeal muscle repolarization

Although the EGL-19 channel clearly affects the action potentials of both the corpus and terminal bulb muscles, based on the expression pattern and the loss-of-function phenotype, gain-of-function mutations cause a myotonic phenotype only in the terminal bulb. This observation suggests that different mechanisms are involved in the control of action potential duration in these two parts of the pharynx. This notion is also supported by the fact that the corpus always repolarizes before the terminal bulb. It seems possible that the corpus has an intrinsic ability to repolarize earlier than the terminal bulb. To achieve a well-regulated and fast repolarization, other ion channels must participate in the repolarization process. For instance, mutations in a glutamate-gated Cl^- channel, encoded by the *avr-15* gene, cause a delay in muscle repolarization.

AVR-15 is apparently part of the pharyngeal muscle receptor for the neurotransmission from M3 inhibitory motor neurons, which directly affect the repolarization of the corpus but not the terminal bulb (Dent *et al.*, 1997). Therefore, M3 activity could preferentially hasten corpus repolarization. However, M3 transmission alone can not entirely account for the difference, since the terminal bulb still repolarizes later than the corpus when M3 transmission is blocked (Raizen and Avery, 1994). Another channel likely to play a role in the repolarization process is the nematode negative spike K^+ channel, originally characterized by Byerly and Masuda (1979) in the *Ascaris* pharynx (see also Davis *et al*., 1995). A difference in the expression or regulation of activity of this and perhaps other channels could account for the different repolarization timing between parts of the pharynx.

Myotonic mutations in egl-19

The myotonic phenotype of *egl-19* mutants is well explained by slower inactivation kinetics of the muscle Ca^{2+} current, since that Ca^{2+} current is likely to be the major inward current during muscle depolarization. When inactivation of the EGL-19 channel is retarded, the muscle membrane potential would be held depolarized, and the resulting sustained Ca^{2+} influx would prolong muscle contraction. L-type voltage-activated Ca^{2+} channels are known to inactivate by two mechanisms, voltage- and calcium-dependent. These two means of inactivation are thought to operate independently (Hadley and Lederer, 1991).

By assaying the inactivation kinetics of chimeric channels (made between an α_{1A} and a marine ray homolog of the α_{1E} class) in *Xenopus* oocytes, Zhang *et al.* (1994) found that a region of the proteins that includes IS6 and flanking residues is responsible for the different rates of voltage-dependent inactivation in voltage-activated Ca^{2+} channels. These authors also suggested that this type of inactivation is reminiscent of the C-type (slow) inactivation observed in voltage-activated K^+ channels, revealed after the removal of N-type (fast) inactivation by deletion of residues that form the tethered plug to the channel pore (Hoshi *et al*., 1991). Recently, a mutation (N434A) in IS6 of the rat μ1 Na^+ channel protein has also been found to affect the slow inactivation of the channel (Wang and Wang, 1997). Two of *egl-19* myotonic mutations, *n2368sd* and *ad952*, are in the IS6 region. We believe that the myotonic phenotype observed in these mutants is caused by a defective voltage-dependent inactivation of the EGL-19 channel. Thus our data extend the importance of the IS6 region in controlling channel inactivation to L-type channels.

The third myotonic mutation, *ad695sd*, is in IIIS4. S4 segments are thought to be the voltage sensors for voltage-sensitive channels (Catterall, 1995). Indeed, an R→H mutation in IIIS4 causes the reduced rate of depolarization observed in *n582* mutants, as would be expected if this mutation affected the voltage sensor of the channel. It is possible that the A→V mutation in IIIS4 found in *ad695sd* animals also affects the activation of the channel. However, we have not observed significantly slowed-down depolarization kinetics in *ad695sd*, in contrast to the dramatically prolonged plateau phases in mutant muscle action potentials. Although the kinetics of channel activation can affect the kinetics of inactivation, it seems unlikely that *ad695sd* mutant channels inactivate slowly simply as a consequence of slow activation kinetics. Thus, the mutation apparently uncouples the role of IIIS4 in channel activation from its role in inactivation. A similar phenomenon has been reported for mutations in the IVS4 segment in vertebrate skeletal muscle Na^+ channels. R1448C and R1448H mutations in the α subunit of the human skeletal muscle voltage-activated Na^+ channel gene SCN4A cause paramyotonia congenita. When the biophysical properties of the channels were assayed in a cell line, it was found that the mutations have only a small effect on activation but dramatically slow inactivation (Chahine *et al*., 1994).

The two myotonic mutations in the IS6 region of the EGL-19 channel may also affect the activation phase of muscle action potentials. First, *n2368sd* has a cold-sensitive Pat phenotype (Table I and Materials and methods). This phenotype is apparently caused by a reduction in gene function, since it is recessive to the wild-type allele and is not complemented by other Pat alleles. How the *n2368sd* mutation imparts this phenotype is not clear. A possibility is that the G→R mutation in IS6 alters the structure of the protein only slightly at high temperatures (~20°C) to affect channel inactivation, whereas the mutation destablizes the protein dramatically at low temperatures (~12°C) to impair channel formation or function. Second, we have noticed in intracellular records that *n582 ad952* double mutants have consistently faster depolarization kinetics than *n582* single mutants (unpublished observations). Since we do not have the *ad952* mutation in isolation, we do not know if the suppression between *n582* and *ad952* is mutual. It should be interesting to assay the detailed biophysical properties of each of these mutant channel proteins in a simpler and more electrophysiologically accessible system, e.g. *Xenopus* oocytes.

In conclusion, our analysis of myotonic mutants in *C.elegans* has implicated a voltage-activated Ca^{2+} channel in regulating the duration of muscle action potentials. Our *in vivo* analysis suggests that mutations in IS6 and IIIS4 regions of the α1 subunit can dramatically affect Ca^{2+} channel inactivation. We envisage that continued genetic analysis of *C.elegans* pharyngeal excitation will further our understanding of the molecular mechanisms that underlie the control of action potential duration in excitable cells.

Materials and methods

General methods

Worm culture, handling and genetic manipulation followed the methods described by Sulston and Hodgkin (1988). Except for cold-sensitivity experiments, all worms were maintained at 20°C. The wild type was the N2 strain of the Bristol variety of *C.elegans*. Methods used for analyzing pharyngeal behavior and electrical activity have been described elsewhere: timing diagrams by Avery (1993); EPGs by Raizen and Avery (1994); and intracellular recordings by Davis *et al.* (1995).

Mutant isolation and genetic characterization

All mutagenesis was carried out with ethyl methanesulfonate (EMS), which causes primarily G:C→A:T transitions (Anderson, 1995). Mutants isolated were backcrossed at least twice against N2 or *bli-6*(*sc16*) *unc-24*(*e138am*) animals.

n2368sd. Mutagenized *egl-1*(*n986dm*) V males were crossed with *unc-79*(*e1068*) *ced-4*(*n1162*) III; *rol-4*(*sc8*) *unc-76*(*e911*) V; *lon-2*(*e678*) *xol-*

1(*y70*) X hermaphrodites. Most viable progeny from this cross should be hermaphrodites with the genotype *unc-79 ced-4*/+; *rol-4 unc-76*/*egl-1*; *lon-2 xol-1*/+ since the *xol-1* mutation kills the male progeny which do not have a wild-type copy of the X chromosome. These hermaphrodites have an egg-laying defective phenotype, since the *egl-1* mutation dominantly causes death of the HSN motor neurons (Trent *et al*., 1983). Two F1 animals showed normal egg-laying among 14 000 scored. One carried *n2368sd* and the other a new *ced-4* allele (Ellis and Horvitz, 1986). We found that the HSNs were still absent in *n2368sd; egl-1*(*n986dm*) double-mutant animals (data not shown) but the egg-laying muscles were now able to contract.

n2368sd was mapped to LGIV between *unc-24* and *bli-6* by two- and three-factor crosses. *n2368sd* is tightly linked to *ad695sd*, since in Unc non-Bli recombinants segregated from *bli-6*(*sc16*) *egl-19*(*ad695sd*) *unc-24*(*e138am*)/*egl-19*(*n2368sd*) either *ad695sd* (10/12) or *n2368sd* (2/12) was present. This result suggests that *n2368sd* and *ad695sd* are no more than 0.5 map units apart. We found no wild-type recombinants among 12 800 progeny segregated from *n2368sd*/*n582* heterozygote mothers. This result indicates that the *n2368sd* mutation can be no more than 0.05 map units (roughly 50 kb) from *n582*. *egl-19*(*n582*) was isolated by Trent *et al*. (1983) for its egg-laying defective phenotype.

Loss-of-function mutations. New loss-of-function mutations were isolated by non-complementation screens against *n582*. Either mutagenized N2 males were crossed with *bli-6*(*sc16*) *egl-19*(*n582*) *unc-24*(*e138am*) hermaphrodites, or mutagenized N2 hermaphrodites were crossed with *bli-6*(*sc16*) *egl-19*(*n582*) *unc-24*(*e138am*)/+ males. Cross progeny were scored for the Egl-19 phenotype. Twelve independent new alleles were isolated from a total of 6 900 haploid genomes screened. Each was within 3 map units of *n582*.

Since five of these 12 *egl-19* mutants had a Pat phenotype similar to that of *pat-5* mutants and since *pat-5* maps close to *egl-19* (Williams and Waterston, 1994), we tested whether *egl-19* and *pat-5* are the same gene. None of four *pat-5* alleles (*st553*, *st556*, *st569* and *st571*) complemented *egl-19*(*n582*). These results and the fact that *pat-5*(*st556*) was rescued by the same cosmid that rescued *egl-19* (see below) suggest that *pat-5* is *egl-19*. We believe that Pat is the null phenotype of *egl-19* because the most severe Pat alleles behave like a chromosomal deletion (a bona fide null) in heterozygotes. For example, *n582*/*nDf41* animals did not show a more severe phenotype than *n582*/*ad1004* animals.

egl-19(*n582*) was mapped previously between *unc-8* and *dpy-20*, near the position +3.4 on chromosome IV (Trent *et al*., 1983). To map further *egl-19*(*n582*), we isolated recombinants from a strain of the genotype *unc-44*(*e362*) *deb-1*(*st555*) *unc-24*(*e138*) / *egl-19*(*n582*). Eleven out of 24 Unc-24 non-Deb recombinants carried *egl-19*(*n582*). This result places *egl-19* approximately half-way between *deb-1* (position +3.3) and *unc-24* (position +3.5), which are approximately 800 kb apart on the physical map (Coulson *et al*., 1995). Since *nDf41* deletes *egl-19* and has its right breakpoint near or within *dif-1* (position +3.4; J.Ahringer, personal communication), *egl-19* must be close to or to the left of *dif-1*, which is ~400 kb from *deb-1*. Together, these results place *egl-19* in an approximately 150 kb interval to the left of *dif-1*.

cis-acting suppressors of n2368sd and ad695sd. We used a genetic *cis-trans* test to establish that the myotonic mutations are alleles of *egl-19*. We introduced *egl-19*(null)-like mutations in *cis* to *n2368sd* (Table 1). The rationale is that if a gain-of-function and a null mutation are in the same gene, the null mutation should occlude the expression of the gain-of-function if these two mutations exist in the *cis* configuration, but not when they are in the *trans* configuration. We made *egl-19*(null) mutations in *cis* to *n2368sd* by non-complementation screens. We crossed mutagenized *n2368sd* hermaphrodites with *bli-6*(*sc16*) *egl-19*(*n582*) *unc-24*(*e138am*)/+ males. One Egl mutant (allele *ad1023*) was isolated among 750 haploid genomes screened. *egl-19* mutations were introduced onto the *ad695sd* mutant chromosome by a similar non-complementation scheme. Among 3 600 mutagenized haploid genomes screened, three alleles (*ad1000*, *ad1002* and *ad1021*) were isolated as Egl mutants. Each of these four new mutations was tightly linked (within 3 map units) to the original semi-dominant allele, *n2368sd* or *ad695sd*, respectively. All of these double mutants were wild type as heterozygotes. In contrast, both *n2368sd* and *ad695sd*, when heterozygous with an *egl-19*(null) mutant chromosome, caused a myotonic phenotype. All five double-mutants were Pat as homozygotes. Thus, *egl-19*(null) mutations are *cis*-dominant *trans*-recessive suppressors of *n2368sd* and *ad695sd*. We conclude that *n2368sd* and *ad695sd* are mutations of *egl-19*.

ad952. We screened for non-Egl F1 progeny of mutagenized *egl-19*(*n582*) hermaphrodites. One such mutant (*ad952 n582*) was found among 15 000 haploid genomes. *ad952* was tightly linked to *n582* and mapped between *bli-6* and *unc-24*, which are ~1 map unit apart.

Tests for cold sensitivity

Gravid hermaphrodites were kept on petri plates in a box placed in a circulating cold water bath in order to maintain a tightly controlled temperature for the embryos. *n2368sd* embryos were nearly 100% Pat at 12°C. Only a small fraction were affected when grown at 15°C. We found no cold sensitivity for *ad695sd*, *n582* or N2 animals.

cDNA cloning and sequencing

General cloning methods followed those described by Sambrook *et al.* (1989). For sequencing, we used an ABI 377 automatic sequencer. For sequence management, we used the GCG Wisconsin Package.

Degenerate PCR primers were designed based on the conserved sequences in the IIIS6 and IVS6 domains of the α1 subunits of vertebrate L-type voltage-activated Ca^{2+} channel genes (primer sequences available upon request). A 953 bp PCR product was amplified from worm cDNA and cloned (pCAC1-953). The cDNA was localized in the genome by hybridizing CAC1–953 to a YAC poly-grid, poly 1 (kindly provided by R.Waterston; Coulson *et al*., 1988). Only two overlapping YAC clones, Y51C8 and Y49F12, showed positive hybridization. Three cosmid clones, C48A7, B0496, and K11C12 (kindly provided by Alan Coulson), together span the overlap of the YACs. By Southern hybridization, we found that CAC1–953 is contained entirely in C48A7, partially in B0496, but not in K11C12. C48A7 has been placed between two genes *deb-1* and *dif-1* on the physical map (Coulson *et al*., 1995).

Using pCAC1–953 as a probe, we screened a mixed-stage worm cDNA library (Barstead and Waterston, 1989) to isolate a 2.8 kb cDNA clone (pCE12A). We then designed PCR primers based on the sequences in pCE12A (TTATTTTGGAATGTAACGATAACGAAACCT) and in the genomic sequence of cosmid C48A7 (provided by the *C.elegans* sequence consortium) corresponding to the first predicted transmembrane domain (IS6) of the Ca^{2+} channel gene (CTTTGCCTCTCCTTGAATAAT-CCCATCCGA) to RT–PCR more 5′cDNA sequence from a cDNA mix made from mixed-stage poly-A selected total RNA. A 3 kb PCR product (e12-RT1) was cloned and sequenced. To obtain further 5′ sequence, we used the Genefinder program (P.Green, unpublished; cited in Eeckman and Durbin, 1995) to help us identify the possible initiating ATG from the genomic sequence. We used a primer corresponding to the sequence immediately 5′ to the ATG (GGAGTGCGCCGACACTGCTCGAT-CGTGA) and another primer corresponding to the 5′ portion of e12-RT1 (TACTCCTGATACAAGACGAAGCGGT) to PCR-amplify a 0.7 kb product from a cDNA mix. The sequence of the PCR product was determined by direct sequencing. pCE12A lacked the poly-A signal sequence, suggesting incomplete 3′ extension. A cDNA clone (yk53d3), isolated and kindly given to us by Yuji Kohara, overlaps in sequence with pCE12A and extends 0.5 kb further 3′ to include the AATAAA poly-A signal. When assembled together, these four pieces would make one 6.2 kb cDNA. The authenticity of this presumptive transcript was verified by RT–PCR using the most 5′ and 3′ primers. A single product of the predicted size was amplified. Based on Northern blots using CAC1-953 as the probe, the full-length transcript should be ~7 kb long. Nevertheless, we believe that the entire ORF is in our sequence, since there are stop codons in all three frames preceding the first in-frame ATG and following the last predicted amino acid.

Isolation of genomic lambda phage clones and germline transformation

We used CAC1-953 as a probe to screen a *C.elegans* genomic lambda FIXII phage library (Stratagene). The sizes and extents of the inserts in phage clones that we isolated were determined by restriction pattern analysis and by direct sequencing of the ends using primers corresponding to the multiple cloning site of the vector. We were able to map these clones precisely, since the sequence of cosmid C48A7 became available during the course of our analysis.

The ability of these phage clones and of C48A7 to rescue *egl-19* mutants was determined by germline transformation experiments (Mello *et al*., 1992). The genomic clone was co-injected into *egl-19*(*n582*) animals with pRAK3, which contains a dominant *rol-6* marker (Mello *et al*., 1992; Davis *et al*., 1995). Transgenic lines that stably expressed the marker were established and observed for Egl-19 defects, including abnormal egg-laying, body morphology, movement and pharyngeal pumping. For C48A7, two of eight lines showed rescue; for F2 and F3 co-injection, five of five; for F2 alone, six of eight; for E3, zero of three; for H1, none of nine; for E2, nine of nine.

Some unusual phenomena associated with the F2 and E2 transgenes

are worth noting. We have observed occasional terminal bulb muscle relaxation defects in some transgenic animals carrying the F2 clone, while their sisters (also transgenic) appeared to be wild type. This variability may reflect the fact that F2 contains an *egl-19* gene truncated at the 3′ end (see Figure 4). Rescue of *egl-19*(*n582*) by E2 transgenes was incomplete. In particular, the egg-laying defective phenotype was only slightly improved in all E2 transgenic animals, whereas pharyngeal and body muscle phenotypes were fully rescued. This result suggests that E2 may lack important regulatory elements for proper expression in egg-laying muscles. This hypothesis could explain why the *egl-19*::*GFP* reporter was not expressed in egg-laying muscles, as the *egl-19* regulatory sequence in the reporter was from E2 (see below and Figure 4).

One transgene carrying C48A7 also rescued an embryonic lethal allele, *st556* (Williams and Waterston, 1994). Males of the genotype *egl-19*(*st556*)/*unc-82*(*e1323*) *unc-24*(*e138am*) IV (a gift from B.Williams) were crossed with the transgenic line *egl-19*(*n582*) IV; *adEx1058*[*egl-19*+ *rol-6*(*d*)]. Viable and sometimes fully wild-type (except for the Rol phenotype of the co-injected *rol-6*(*d*) gene) animals were segregated of the genotype *egl-19*(*st556*) IV; *adEx1058*[*egl-19*(+) *rol-6*(*d*)].

Mutation detection

Genomic DNA was prepared from animals homozygous for the respective mutations. Segments of the *egl-19* gene were amplified by PCR. The sequences of the entire coding regions and intron–exon boundaries from *ad695sd*, *n2368sd* and *n582 ad952* animals were determined by direct sequencing of PCR products. The sequences were compared to the genomic sequence of the C48A7 cosmid made available by the *C.elegans* Genome Consortium. Wherever a suspected mutation was found, the sequencing was repeated at least once more to eliminate potential artifacts. The sequences of the oligonucleotides used for amplification and/or sequencing of the exons are available upon request.

egl-19::GFP fusion

A translational fusion of *egl-19* and *GFP* was made by inserting a 4.7 kb fragment of *egl-19* into the multiple cloning site in the pPD95.70 *GFP* expression vector (A.Fire, J.Ahnn, G.Seydoux and S.Xu, personal communication), which also contains a nuclear localization signal. The *egl-19* fragment was prepared from phage E2 (see Figure 4). E2 DNA was digested with *Bcg*I. The open ends were blunted by Klenow enzyme. E2 was then digested again with *Sal*I, which cuts in the vector. The 4.7 kb fragment was gel-purified. The pPD95.70 vector was prepared by digestion with *Sma*I and *Sal*I followed by gel purification. Ligation of these two fragments resulted in fusion of the *egl-19* translation frame to that of the *GFP*. The fusion construct (peat-12::sGFP-NLS) was cloned and checked by restriction digests and used to germline transform *lin-15*(*n765ts*) animals along with DA#735 (a plasmid containing *lin-15*; Huang *et al*., 1994) as a co-injection marker. Transmitting lines that segregated wild-type animals were established and the expression of *GFP* was observed in wild-type animals by fluorescence microscopy with an FITC filter set. We had 10 independent lines expressing *egl-19*::*GFP*, and they looked essentially the same with respect to where the signal was detected. The strength of the signal, however, varied widely among them. We therefore concentrated our further analysis on the line that had the strongest expression. We present (in Figure 5) a view of the pharynx in a dauer animal, because the expression pattern of *egl-19*::*GFP* in the pharynx is most easily photographed in dauers, as the pharynx is flat and compact.

Acknowledgements

We thank the *C.elegans* Genome Consortium for cosmid sequences, A.Coulson for cosmids, Y.Kohara for a partial cDNA clone of *egl-19*, A.Fire for *GFP* expression vectors, R.Waterston for YAC filters, B.Williams for *pat-5* mutant strain, and K.S.Liu and J.A.Dent for sharing unpublished results. Some strains used in mapping experiments were supplied by the Caenorhabditis Genetics Center, which is supported by the National Institute of Health National Center for Research Resources. We also thank M.W.Davis, J.A.Dent, R.Joho, F.Katz, D.Raizen and R.Zwaal for their constructive comments on the manuscript. This research was supported by United States Public Health Service research grants HL46154 to L.Avery and GM24663 to H.R.Horvitz. H.R.H. is an Investigator at the Howard Hughes Medical Institute.

References

Albertson,D.G. and Thomson,J.N. (1976) The pharynx of *Caenorhabditis elegans*. *Phil. Trans. R. Soc. Lond.*, **B275**, 299–325.

Anderson,P. (1995) Mutagenesis. In Epstein,H.F. and Shakes,D.C. (eds), *Methods in Cell Biology, Caenorhabditis elegans: Modern Biological Analysis of an Organism*. Academic Press, Inc., San Diego, CA, Vol. 48, pp. 31–58.

Avery,L. (1993) The genetics of feeding in *Caenorhabditis elegans*. *Genetics*, **133**, 897–917.

Avery,L. and Horvitz,H.R. (1989) Pharyngeal pumping continues after laser killing of the pharyngeal nervous system of *C. elegans*. *Neuron*, **3**, 473–485.

Barstead,R.J. and Waterston,R.H. (1989) The basal component of the nematode dense-body is vinculin. *J. Biol. Chem*., **264**, 10177–10185.

Bean,B.P. (1989) Classes of calcium channels in vertebrate cells. *Annu. Rev. Physiol*., **51**, 367–384.

Byerly,L. and Masuda,M.O. (1979) Voltage-clamp analysis of the potassium current that produces a negative-going action potential in *Ascaris* muscle. *J. Physiol. Lond*., **288**, 263–284.

Catterall,W.A. (1995) Structure and function of voltage-gated ion channels. *Annu. Rev. Biochem*., **64**, 493–531.

Chahine,M., George,A.L.,Jr., Zhou,M., Ji,S., Sun,W., Barchi,R.L. and Horn,R. (1994) Sodium channel mutations in paramyotonia congenita uncouple inactivation from activation. *Neuron*, **12**, 281–294.

Chalfie,M., Tu,Y., Euskirchen,G., Ward,W.W. and Prasher,D.C. (1994) Green fluorescent protein as a marker for gene expression. *Science*, **263**, 802–805.

Coulson,A., Waterston,R., Kiff,J., Sulston,J. and Kohara,Y. (1988) Genome linking with yeast artificial chromosomes. *Nature*, **335**, 184–186.

Coulson,A., Huynh,C., Kozono,Y. and Shownkeen,R. (1995) The physical map of the *Caenorhabditis elegans* genome. In Epstein,H.F. and Shakes,D.C. (eds), *Methods in Cell Biology, Caenorhabditis elegans: Modern Biological Analysis of an Organism*. Academic Press, Inc., San Diego, CA, Vol. 48, pp. 533–550.

Curran,M.E., Splawski,I., Timothy,K.W., Vincent,G.M., Green,E.D. and Keating,M.T. (1995) A molecular basis for cardiac arrhythmia: HERG mutations cause long QT syndrome. *Cell*, **80**, 795–803.

Davis,M.W., Somerville,D., Lee,R.Y.N., Lockery,S., Avery,L. and Fambrough,D.M. (1995) Mutations in the *Caenorhabditis elegans* Na,K-ATPase α-subunit gene, *eat-6*, disrupt excitable cell function. *J. Neurosci*., **15**, 8408–8418.

de Leon,M., Wang,Y., Jones,L., Perez-Reyes,E., Wei,X., Soong,T.W., Snutch,T.P. and Yue,D.T. (1995) Essential Ca^{2+}-binding motif for Ca^{2+}-sensitive inactivation of L-type Ca^{2+} channels. *Science*, **270**, 1502–1506.

Dent,J.A., Davis,M.W. and Avery,L. (1997) *avr-15* encodes a chloride channel subunit that mediates inhibitory glutamatergic neurotransmission and ivermectin sensitivity in *C.elegans*. *EMBO J*., in press.

Eeckman,F.H. and Durbin,R. (1995) ACeDB and Macace. In Epstein,H.F. and Shakes,D.C. (eds), *Methods in Cell Biology, Caenorhabditis elegans: Modern Biological Analysis of an Organism*. Academic Press, Inc., San Diego, CA, Vol. 48, pp. 583–605.

Ellis,H.M. and Horvitz,H.R. (1986) Genetic control of programmed cell death in the nematode *C. elegans*. *Cell*, **44**, 817–829.

Grabner,M., Friedrich,K., Knaus,H.-G., Striessnig,J., Scheffauer,F., Staudinger,R., Koch,W.J., Schwartz,A. and Glossmann,H. (1991) Calcium channels from *Cyprinus carpio* skeletal muscle. *Proc. Natl Acad. Sci. USA*, **88**, 727–731.

Grabner,M., Wang,Z., Hering,S., Striessnig,J. and Glossmann,H. (1996) Transfer of 1,4-dihydropyridine sensitivity from L-type to class A (BI) calcium channels. *Neuron*, **16**, 207–218.

Hadley,R.W. and Lederer,W.J. (1991) Ca^{2+} and voltage inactivate Ca^{2+} channels in guinea-pig ventricular myocytes through independent mechanisms. *J. Physiol. Lond*., **444**, 257–268.

Hall,D.H. and Hedgecock,E.M. (1991) Kinesin-related gene *unc-104* is required for axonal transport of synaptic vesicles in *C. elegans*. *Cell*, **65**, 837–847.

Hochner,B., Klein,M., Schacher,S. and Kandel,E.R. (1986) Action-potential duration and the modulation of transmitter release from the sensory neurons of *Aplysia* in presynaptic facilitation and behavioral sensitization. *Proc. Natl Acad. Sci. USA*, **83**, 8410–8414.

Hodgkin,J. (1988) Sexual dimorphism and sex determination. In Wood,W.B. and the Community of *C. elegans* Researchers (eds), *The Nematode Caenorhabditis elegans*. Cold Spring Harbor Laboratory Press, Cold Spring Harbor, NY, pp. 243–279.

Hoshi,T., Zagotta,W.N., and Aldrich,R.W. (1991) Two types of inactivation in Shaker K^+ channels: effects of alterations in the carboxy-terminal region. *Neuron*, **7**, 547–556.

Huang,L.S., Tzou,P. and Sternberg,P.W. (1994) The *lin-15* locus encodes two negative regulators of *Caenorhabditis elegans* vulval development. *Mol. Biol. Cell*, **5**, 395–411.

Huizinga,J.D. (1991) Action potentials in gastrointestinal smooth muscle. *Can. J. Physiol. Pharmacol.*, **69**, 1133–1142.

Kass,R.S. (1995) Ionic basis of electrical activity in the heart. In Sperelakis,N. (ed.), *Physiology and Pathophysiology of the Heart*. 3rd edn. Kluwer Academic Publishers, Norwell, MA, pp. 77–90.

Mello,C.C., Kramer,J.M., Stinchcomb,D. and Ambros,V. (1992) Efficient gene transfer in *C. elegans*: extrachromosomal maintenance and integration of transforming sequences. *EMBO J.*, **10**, 3959–3970.

Mikami,A., Imoto,K., Tanabe,T., Niidome,T., Mori,Y., Takeshima,H., Narumiya,S. and Numa,S. (1989) Primary structure and functional expression of the cardiac dihydropyridine-sensitive calcium channel. *Nature*, **340**, 230–233.

Mori,Y. *et al.* (1991) Primary structure and functional expression from complementary DNA of a brain calcium channel. *Nature*, **350**, 398–402.

Niidome,T., Kim,M.S., Friedrich,T. and Mori,Y. (1992) Molecular cloning and characterization of a novel calcium channel from rabbit brain. *FEBS Letters*, **308**, 7–13.

Noble,D. (1979) *The Initiation of the Heart Beat*. 2nd edn. Oxford University Press, New York.

Raizen,D.M. and Avery,L. (1994) Electrical activity and behavior in the pharynx of *Caenorhabditis elegans*. *Neuron*, **12**, 483–495.

Riddle,D.L. (1988) The dauer larva. In Wood,W.B. and the Community of *C. elegans* Researchers (eds), *The Nematode Caenorhabditis elegans*. Cold Spring Harbor Laboratory Press, Cold Spring Harbor, NY, pp. 393–412.

Sambrook,J., Fritsch,E.F. and Maniatis,T. (1989) *Molecular Cloning. A Laboratory Manual*. Cold Spring Harbor Laboratory Press, Cold Spring Harbor, NY.

Schafer,W.R. and Kenyon,C.J. (1995) A calcium-channel homologue required for adaptation to dopamine and serotonin in *Caenorhabditis elegans*. *Nature*, **375**, 73–78.

Schafer,W.R., Sanchez,B.M. and Kenyon,C.J. (1996) Genes affecting sensitivity to serotonin in *Caenorhabditis elegans*. *Genetics*, **143**, 1219–1230.

Schwartz,P.J., Locati,E.H., Napolitano,C. and Priori,S.G. (1995) The long QT syndrome. In Zipes,D.P. and Jalife,J. (eds), *Cardiac Electrophysiology: From Cell to Bedside*. W.B. Sanders Company, Philadelphia, PA, pp. 788–811.

Spencer,A.N., Przysienzniak,J., Acosta-Urquidi,J. and Basarsky,T.A. (1989). Presynaptic spike broadening reduces junctional potential amplitude. *Nature*, **340**, 636–638.

Starich,T.A., Lee,R.Y.N., Panzarella,C., Avery,L. and Shaw,J.E. (1996) *eat-5* and *unc-7* represent a multigene family in *Caenorhabditis elegans* involved in cell–cell coupling. *J. Cell Biol.*, **134**, 537–548.

Sulston,J. and Hodgkin,J. (1988) Methods. In Wood,W.B. and the Community of *C.elegans* Researchers (eds), *The Nematode Caenorhabditis elegans*. Cold Spring Harbor Laboratory Press, Cold Spring Harbor, NY, pp. 587–606.

Trent,C., Tsung,N. and Horvitz,H.R. (1983). Egg-laying defective mutants of the nematode *Caenorhabditis elegans*. *Genetics*, **104**, 619–647.

Wang,Q., Shen,J., Splawski,I., Atkinson,D., Li,Z., Robinson,J.L., Moss,A.J., Towbin,J.A. and Keating,M.T. (1995) SCN5A mutations associated with an inherited cardiac arrhythmia, long QT syndrome. *Cell*, **80**, 805–811.

Wang,S.-Y. and Wang,G.K. (1997) A mutation in segment I-S6 alters slow inactivation of sodium channels. *Biophys. J.*, **72**, 1633–1640.

Warmke,J.W. and Ganetzky,B. (1994) A family of potassium channel genes related to *eag* in *Drosophila* and mammals. *Proc. Natl Acad. Sci. USA*, **91**, 3438–3442.

Williams,M.E., Brust,P.F., Feldman,D.H., Patthi,S., Simerson,S., Maroufi,A., McCue,A.F., Velicelebi,G., Ellis,S.B. and Harpold,M.M. (1992a) Structure and functional expression of an omega-conotoxin-sensitive human N-type calcium channel. *Science*, **257**, 389–395.

Williams,M.E., Feldman,D.H., McCue,A.F., Brenner,R., Velicelebi,G., Ellis,S.B. and Harpold,M.M. (1992b) Structure and functional expression of $\alpha 1$, $\alpha 2$, and β subunits of a novel human neuronal calcium channel subtype. *Neuron*, **8**, 71–84.

Williams,B.D. and Waterston,R.H. (1994) Genes critical for muscle development and function in *Caenorhabditis elegans* identified through lethal mutations. *J. Cell Biol.*, **124**, 475–490.

Wilson,R. *et al.* (1994) 2.2 Mb of contiguous nucleotide sequence from chromosome III of *C. elegans*. *Nature*, **368**, 32–38.

Zhang,J.-F., Ellinor,P.T., Aldrich,R.W. and Tsien,R.W. (1994) Molecular determinants of voltage-dependent inactivation in calcium channels. *Nature*, **372**, 97–100.

Zhong,Y. and Wu,C.-F. (1991) Alteration of four identified K^+ currents in *Drosophila* muscle by mutations in *eag*. *Science*, **252**, 1562–1564.

Received on April 1, 1997; revised on July 18, 1997